Preprints of the 12th IFAC Symposium on Computer Applications in Biotechnology
The International Federation of Automatic Control
16-18, 2013, December. Mumbai, India

Modelling light-dark regime influence on the carbon-nitrogen metabolism in a unicellular diazotrophic cyanobacterium

Ghjuvan Micaelu Grimaud [*,⋆] **Anthony Dron** [**,***]
Sophie Rabouille [**,***] **Antoine Sciandra** [**,***]
Olivier Bernard [*,⋆]

[*] *BIOCORE-INRIA, BP93, 06902 Sophia-Antipolis Cedex, France*
[**] *UPMC Univ Paris 06, UMR 7093, LOV, Observatoire oceanologique, F-06234, Villefranche/mer, France*
[***] *CNRS, UMR 7093, LOV, Observatoire oceanologique, F-06234, Villefranche/mer, France*

Abstract: We propose a dynamical model depicting nitrogen (N_2) fixation (diazotrophy) in a unicellular cyanobacterium, *Crocosphaera watsonii*, grown under light limitation and obligate diazotrophy. In this model, intracellular carbon and nitrogen are both divided into a structual pool and a storage pool. An internal pool that explicitly describes the nitrogenase enzyme is also added. The model is successfully validated with continuous culture experiments of *C. watsonii* under three light regimes, indicating that proposed mechanisms accurately reproduce the growth dynamics of this organism under various light environments. Then, a series of model simulations is run for a range of light regimes with different photoperiods and daily light doses. Results reveal how nitrogen and carbon are coupled, through the diel cycle, with nitrogenase dynamics, whose activity is constrained by the light regime. We finally identify optimal productivity conditions.

Keywords: dynamic modelling, cyanobacteria, light regime, optimum

1. INTRODUCTION

Nitrogen-fixing cyanobacteria (diazotrophs) are important actors of biogeochemical cycles in (sub)-tropical oceans (Karl et al., 2002), where they can be responsible of 20 to 40 % of the new primary production (Lee et al., 2002). The conspicuous, colonial cyanobacteria (*Trichodesmium* spp. (Carpenter and Romans, 1991)) were considered as the dominant marine diazotrophs, until the importance of unicellular N_2-fixing cyanobacteria (UCYN, such as *Crocosphaera watsonii* Waterbury and Rippka (1989)) was pointed-out (Zehr et al., 2001). UCYN now prove widely abundant and active in the nitrogen cycle (Zehr et al., 2011).

These newly discovered nitrogen fixing cyanobacteria have a strong potential for biotechnological applications. They might provide nitrogen to microorganisms of interest, offering the economical and ecological alternative to the use of fertilizers. However, if UCYN are now more intensively studied, their physiology and the influence of physicochemical factor such as temperature or light remain poorly known. Understanding nitrogen fixation dynamics in cultivated UCYN is a pre-requisite to the development of such applications.

Carbon-nitrogen metabolism and growth in photoautotrophic organisms are constrained by environmental factors, such as light availability or photoperiod length. Owing to the O_2-sensitivity of the N_2-fixing nitrogenase enzyme (Robson and Postgate, 1980), carbon and nitrogen acquisition in the UCYN *C. watsonii* are separated in time: N_2 fixation is mainly restricted to the dark period when oxygenic photosynthesis does not occur (Mitsui et al., 1986). Such temporal segregation is allowed by carbon storage as carbohydrates. In order to study the coupling between photosynthesis and diazotrophy in *C. watsonii*, an experimental study was carried out with various photoperiod lengths (Dron et al., 2012a,b, 2013). On the basis of these experiments, we propose here a dynamical model of diazotrophy in the unicellular cyanobacterium *C watsonii*. We tackle the effect of photoperiod length and daily light dose on the carbon-nitrogen coupling, and we identify conditions leading to an optimal combination for carbohydrates storage, nitrogen fixation and total biomass.

⋆ Corresponding authors {ghjuvan.grimaud, olivier.bernard}@inria.fr

2. MATERIAL AND METHODS

2.1 Experimental approach

Experimental procedure is described in Dron et al. (2012a) and it is only briefly recalled here. Duplicate continuous cultures were maintained under three different photoperiod lengths (12:12, 16:8 and 8:16 light:dark conditions. In all three light regimes, the irradiance followed a truncated sinusoidal cycle with a maximum irradiance of 130 μmol quanta m^{-2} s^{-1}.

2.2 Model design

The present mathematical model is designed to represent the coupling between carbon and nitrogen metabolism, in order to analyze how photoperiodism affects nitrogen assimilation. The experiments devoted to validate the model were conducted under conditions of light-dark cycle and of obligate diazotrophy. We focus on the growth of *C. watsonii* in terms of total organic carbon C_{tot} (biomass), and all considered variables are bulk concentrations.

In line with Rabouille et al. (2006), Ross and Geider (2009) and Mairet et al. (2010), we consider that organic carbon can be split into structural, storage and enzymatic pools. While the structural pool C_f includes membranes, nucleic acids and all proteins (except the nitrogenase), the storage pool C_{st} includes both small metabolites derived from photosynthesis and carbohydrate reserves. Last, the enzymatic pool C_{nit} represents active nitrogenase enzyme, expressed by its carbon content. In the same way, we consider that cellular nitrogen discriminates between a structural compartment and a storage compartment. The structural compartment N_f includes the same molecules as C_f. We assume constant stoichiometry for the structural compartment. N_f is deduced from C_f using the conversion parameter α_3:

$$N_f = \alpha_3 C_f \tag{1}$$

The storage compartment N_{st} includes the first products of N_2 fixation, mainly glutamine (Carpenter and Capone, 1992), and nitrogen reserve components such as cyanophycin (Li et al., 2001). The total organic nitrogen is denoted N_{tot}. We consider that there is only one inorganic nitrogen source available for growth, N_2, so that diazotrophy is obligate.

Metabolic reaction network is represented in Fig. 1 and can be encapsulated in a set of macroscopic reactions representing mass transfers (Bastin and Dochain, 1990). In the following we detail each considered metabolic reaction.

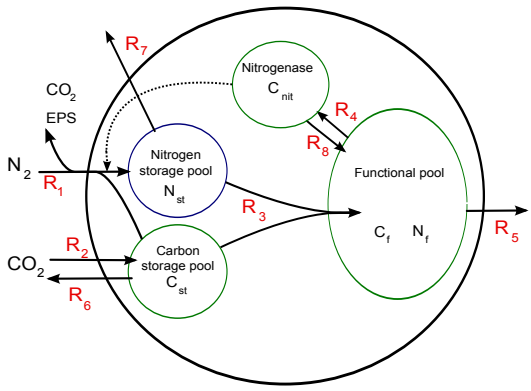

Fig. 1. Conceptual representation of carbon and nitrogen metabolism in *C. watsonii*. Black arrows represent mass fluxes between compartments, dashed arrows represent dependencies links. The different reactions are numbered (R_j). Note that the structural compartment can either be expressed as nitrogen (N_f) or carbon (C_f).

Photosynthesis and reserves build up. During photosynthesis, CO_2 is fixed and transformed into elementary metabolites through the Calvin cycle. Then, these elemental organic carbon compounds are built into carbohydrates. Both processes feed the compartment C_{st}, which thus mainly contains carbohydrates:

$$R_2 : \mathrm{CO_2} \xrightarrow{\rho_2(\mathrm{I(t)},\mathrm{C_f})} \mathrm{C_{st}} \tag{2}$$

This reaction R_2 is dependent upon the structural carbon C_f which contains all the enzymatic apparatus. The carbon fixation rate $\rho_2(I)$, expressed in μmol-C/L/h, follows a Michaelis-Menten kinetics at low light intensity and deals with photoinhibition at high light intensity. This latter phenomenon, which is a slow and reversible reduction of the photosynthetic efficiency at high irradiance (Long et al., 1994), can be described by an Haldane type function when the irradiance changes sufficiently slowly (Han, 2001):

$$\rho_2(I) = r_2 \frac{I(t)}{I(t) + K_I + \dfrac{I^2}{K_{iI}}} C_f \tag{3}$$

where $I(t)$ is the irradiance value at time t, K_I is the half-saturation constant of carbon fixation with respect to light, r_2 is the maximum carbon fixation rate, and K_{iI} is an inhibition coefficient.

Biosynthesis of structral molecules. Structural carbon and nitrogen are metabolized from carbon and nitrogen reserves, through, e.g., protein synthesis. We assume that biosynthesis of structural carbon C_f and structural nitrogen N_f are simultaneous, with a constant C_f/N_f stoichiometry:

$$R_3 : C_{st} + \alpha_3 N_{st} \xrightarrow{\rho_3(N_{st},C_{st})} C_f + \alpha_3 N_f + \mathrm{CO_2} \tag{4}$$

where the specific rate $\frac{\rho_3(N_{st},C_{st})}{C_{st}}$ of reaction R_3 is assumed to be proportional to the available nitrogen N_{st}:

$$\rho_3(N_{st}, C_{st}) = \beta_3 N_{st} C_{st} \tag{5}$$

with β_3 the synthesis rate of structural carbon biosynthesized from C_{st}. Structural nitrogen is synthesized from stored nitrogen N_{st}, concomitantly to the synthesis of structural carbon from C_{st}.

Diazotrophy and nitrogenase synthesis. Nitrogen fixation is an energy consuming process. Required energy is provided by the catabolism of stored carbohydrates (Mitsui et al., 1986).The macroscopic nitrogen balance results from three processes (respiration, nitrogen excretion and N_2 uptake). We thus consider that it relies on the catabolism of C_{st}, which supports the direct costs of N_2 fixation:

$$R_1 : N_2 + \alpha_1 C_{st} \xrightarrow{\rho_1(C_{st},C_{nit})} 2N_{st} + x\mathrm{CO_2} + yC_{\mathrm{excreted}} \tag{6}$$

where C_{excreted} is the fraction of carbon excreted in the form of extracellular polymeric substances (EPS) (Dron et al., 2012b). Also, $x + y = \alpha_1$. All nitrogen fixed is stored into N_{st}. This reaction depends on the compartment C_{nit}, assuming that nitrogenase activity is linearly dependent on nitrogenase quantity. Energy requirements for diazotrophy are fuelled by C_{st}. Therefore, the rate at which N_2 is fixed is taken as a Michaelis-Menten function of C_{st}:

$$\rho_1(C_{st}, C_{nit}) = \gamma_1 \frac{C_{st}}{C_{st} + K} C_{nit} \tag{7}$$

where γ_1 is the maximal rate of N_2 fixation and K is the half-saturation constant of nitrogen fixation.

Because the enzymatic apparatus is included inside C_f, we assume that the nitrogenase is synthesized from C_f:

$$R_4 : C_f \xrightarrow{\rho_4(\phi(t),C_f)} C_{nit} \qquad (8)$$
$$\rho_4(\phi(t), C_f) = \phi(t) r_4 C_f$$

where r_4 is the maximum, specific rate of nitrogenase synthesis. As detailed hereafter, cell-cycle plays a key role in nitrogenase synthesis.

Nitrogenase synthesis and cell-cycle clock. Nitrogenase is synthesized *de novo* each day (Chow and Tabita, 1994) and the rate $\rho_4(\phi(t), C_f)$ of nitrogenase synthesis is assumed to depend on the average position of the cell into its division cycle, represented by the function $\phi(t)$. This function takes into account the circadian clock, adjusted to the maximal irradiance time $T_{I_{max}}$. The use of such time function is motivated by the fact that a highly conserved time pattern was reported in cultures of *C. watsonii* grown under a rather wide range of light regimes (Dron et al., 2013). This cyanobacterium starts cell division close to the mid-light period; the cell division period lasts for 4.5 to 5.5 hours. Nitrogenase activity only appears 4.5 to 6 hours after the onset of cell division. The trigger for nitrogen fixation to start is not the onset of the dark but the completion of cell mitosis. In the end, a constant, 10 to 11 hours delay has been reported between the onset of cell division and the beginning of nitrogenase activity, which could correspond to an incompressible time before cells get ready for nitrogenase activity (genes expression and regulation; Dron et al. (2013)). The mid-light phase is thus a reliable mark from which to count down the time length before nitrogenase becomes active. Also, nitrogen fixation never lasts for more than 12 hours under all light regimes (Dron et al., 2013). Therefore, the function $\phi(t)$ defines a time window in the light cycle when nitrogenase can be synthesized and is active. The time window $\phi(t)$ finally begins 11 hours after the mid light phase and lasts for about 6 hours:

$$\begin{cases} \phi(t) = 1 \\ \text{for t mod } 24 \in (\mathrm{T_{I_{max}}} + 11; \mathrm{T_{I_{max}}} + 17) \\ \phi(t) = 0 \text{ else} \end{cases} \qquad (9)$$

where $T_{I_{max}}$ is the time at which $I(t)$ is maximum.

Due to a daily degradation of the nitrogenase complex, the enzyme concentration decreases as synthesis also stops after a few hours (Chow and Tabita, 1994). The nitrogenase decrease follows a constant, per capita degradation rate, and is proportional to the enzyme concentration :

$$R_8 : C_{nit} \xrightarrow{\rho_8(C_{nit})} C_f \qquad (10)$$
$$\rho_8(C_{nit}) = r_8 C_{nit}$$

where r_8 is the rate of nitrogenase degradation. We assume that the products of nitrogenase degradation are not excreted.

Loss processes. Grosskopf and LaRoche (2012a) reported that *C. watsonii* operates a 'respiratory protection' mechanism to limit nitrogenase inhibition by reducing the intracellular pO_2. We thus considere that respiration of carbon reserves C_{st} further increases when diazotrophy and photosynthesis co-occur, as an indirect cost of diazotrophy. We assume that respiration is then linearly dependent upon photosynthesis, to compensate O_2 production, and also proportional to the rate of N_2 fixation:

$$R_6 : C_{st} \xrightarrow{\rho_6(C_f, I(t), C_{nit}, C_{st})} \mathrm{CO_2} \qquad (11)$$
$$\rho_6(C_{st}) = [\lambda_6 \rho_1(C_{st}, C_{nit}) \rho_2(C_f, I(t)) + r_6] C_{st}$$

where λ_6 is the parameter that takes into account the cost of the co-occurrence of diazotrophy and photosynthesis. We also add a constant respiration term r_6, which accounts for the metabolic maintenance costs.

To embody the excretion of dissolved organic carbon, the structural compartment C_f is degraded at a constant rate β_5:

$$R_5 : C_f + \alpha_3 N_f \xrightarrow{\rho_5(N_f, C_f)} x_{org} \qquad (12)$$
$$\rho_5(N_f) = \beta_5 N_f C_f$$

where x_{org} represents organic molecules excreted as amino acids or proteins. Because N_f and C_f belong to the same molecules, they are degraded simultaneously with a rate of degradation proportional to the N/C stoichiometry of the structural compartment.

Diazotrophic cyanobacteria discharge a significant proportion of the recently fixed N_2 (Mulholland et al., 2004). We therefore represent nitrogen excretion as a constant proportion of the activity of nitrogen fixation, lost from the stored nitrogen N_{st} (reaction R_7), which implies that the higher the fixation rate, the more nitrogen is excreted:

$$R_7 : N_{stock} \xrightarrow{\rho_7(N_{stock})} \mathrm{DON}$$
$$\rho_7(N_{stock}) = r_7 N_{stock} \qquad (13)$$

$$\begin{cases} \dot{C}_{st} = r_2 \dfrac{I(t)}{I(t)+K_I} C_f - \Big[\beta_3 N_{st} + \alpha_1 \dfrac{\gamma_1}{C_{st}+K} C_{nit} \\ \quad + \lambda_6 \rho_1(C_{st}, C_{nit}) \rho_2(C_f, I(t)) + r_6 + D \Big] C_{st} \\ \dot{C}_f = \beta_3 C_{st} N_{st} - (\beta_5 N_f + r_4 \phi(t) + D) C_f \\ \dot{N}_{st} = \gamma_1 \dfrac{C_{st}}{C_{st}+K} C_{nit} - (\alpha_3 \beta_3 C_{st} + r_7 + D) N_{st} \\ \dot{C}_{nit} = r_4 \phi(t) C_f - (r_8 + D) C_{nit} \end{cases} \qquad (14)$$

Model equations are described in the system (14); parameters and state variables are listed in Tab. 1.

The model is run using Matlab® 7.9.0 with the solver ode23 applying Runge-Kutta method.

2.3 Model calibration and sensitivity

All model parameters are estimated but K_I and K_{iI}, and are chosen in agreement with the work of Goebel et al. (2008), who consider that photoinhibition is visible from 600 μE m^2 s^{-1} in *C. watsonii*. The parameters

estimation is performed in the maximum-likelihood sense. The maximum-likelihood estimator is given as:

$$(\hat{\theta}, \hat{\Sigma}) = \arg\min_{\theta,\Sigma} \Big[\frac{n_t}{2} \ln\det\Sigma + \frac{1}{2} \sum_{i=1}^{n_t} \big[y(t_i) - y_m(t_i,\theta)\big]^T \big[y(t_i) - y_m(t_i,\theta)\big] \Big] \quad (15)$$

where $y(t_i)$ is the vector of data collected at time t_i, $y_m(t_i)$ is the vector of data collected at time t_i minus the measurement errors, θ is the parameter vector, $\hat{\theta}$ is the estimated parameter vector, Σ is the covariance matrix of the measurement errors ϵ_i, n_t is the number of observation times and $\hat{\Sigma}$ is the maximum-likelihood estimate of the covariance matrix. We assume that Σ is unknown and diagonal, so that the maximum-likelihood estimator for θ which minimizes the cost function, is:

$$J(\theta) = \sum_{k=1}^{n_y} \frac{n_t}{2} \ln \left[\sum_{\mathrm{i}=1}^{\mathrm{n_t}} \big[\mathrm{y_k(t_i)} - \mathrm{y_{m_k}(t_i,\hat{\theta})}\big]^2 \right] \quad (16)$$

where the maximum-likelihood estimate of the covariance matrix $\hat{\Sigma}$ is:

$$\hat{\Sigma} = \mathrm{diag}(\hat{\sigma}_1^2, \ldots, \hat{\sigma}_{\mathrm{n_y}}^2) \quad (17)$$

$$\text{with} \quad \hat{\sigma}_{\mathrm{k}}^2 = \frac{1}{\mathrm{n_t}} \sum_{\mathrm{i}=1}^{\mathrm{n_t}} \big[\mathrm{y_k(t_i)} - \mathrm{y_{m_k}(t_i,\hat{\theta})}\big]^2 \quad (18)$$

The matlab toolbox IDEAS (Muñoz Tamayo et al., 2009) is used to estimate the model parameters using a maximum-likelihood criterion. The experiment under intermediate photoperiod (12:12 LD regime) is used for the calibration. We compare data sets of POC, PON, carbohydrates and nitrogenase activity to the quantity C_{tot}, N_{tot}, C_{st} and to the nitrogen inflow, respectively. The model is then validated with two other experiments (8:16 and 16:8 LD regimes), using the same parameters set. The fitness between the model and the experimental data is quantified using the coefficient of determination R^2.

A sensitivity analysis is also performed using IDEAS (Muñoz Tamayo et al., 2009) to determine the key parameters and the robustness of the model. The sensitivity analysis is given as a matrix representation of the norm of the normalized sensitivities (A) where the element ($a_{k,j}$) of the matrix is:

$$a_{k,j} = \sum_{i=1}^{n} \left| \frac{\hat{\theta}_j}{y_{m_k}(t_i,\hat{\theta})} \Big[\frac{\partial y_{m_k}}{\partial \theta_j} \Big] \right| \quad (19)$$

with $\hat{\theta}_j$ the j^{th} value of $\hat{\theta}$, y_{m_k} the k^{th} value of y_m.

Sensitivity analysis shows that a small number of parameters strongly impacts the model dynamics under both light regimes. More precisely, some parameters influence a variable in particular. Highest sensitivity is observed in regard to r_2, which controls the inorganic carbon fixation during photosynthesis. It is worth noting that the nitrogen compartment N_{tot} is mostly influenced by the variation of this parameter. Other important parameters are r_4 and r_8, involved in the synthesis and degradation of the nitrogenase enzyme. The parameter γ_1, controlling the respiration of C_{st} for diazotrophy, shows a strong effect on the carbon dynamics, in particular on the carbon stored.

Table 1. Model variables and parameters.

State variables	Unit
C_f, structural carbon pool	$\mu mol[C]\ L^{-1}$
C_{st}, carbohydrates pool	$\mu mol[C]\ L^{-1}$
C_{nit}, nitrogenase pool	$\mu mol[C]\ L^{-1}$
N_{st}, nitrogen storage pool	$\mu mol[N]\ L^{-1}$
Ordinary variables	
N_f, structural nitrogen pool	$\mu mol[N]\ L^{-1}$
C_{tot}, total carbon of *C.watsonii*	$\mu mol[C]\ L^{-1}$
N_{tot}, total nitrogen of *C.watsonii*	$\mu mol[N]\ L^{-1}$
Forcing variables	
$I(t)$, irradiance	$\mu mol\ quanta\ m^{-2}\ s^{-1}$
T, photoperiod	h^{-1}
Parameters	
r_2, CO_2 fixation rate	$0.205\ h^{-1}$
r_4, nitrogenase synthesis rate	$0.006\ h^{-1}$
r_6, respiration of reserves from C_{st}	$0.042\ h^{-1}$
r_7, degradation rate of N_{st}	$0.02\ h^{-1}$
r_8, nitrogenase degradation rate	$0.83\ h^{-1}$
α_1, catabolism of C_{st} for N_2 fixation	$0.25\ \mu mol[C]\mu mol[N]^{-1}$
α_3, N_f synthesis	$0.155\ \mu mol[N]\mu mol[C]^{-1}$
β_3, structural carbon synthesis rate	$0.0006\ \mu mol[N]^{-1}\ L\ h^{-1}$
β_5, degradation rate of C_f	$5.10^{-5}\ \mu mol[N]^{-1}\ L\ h^{-1}$
γ_1, N_2 fixation rate	$16\mu mol[N]\mu mol[C]^{-1}h^{-1}$
λ_6, respiratory protection	$0.022\ \mu mol[C]^{-1}$ $\mu mol[N]^{-1}\ L^2\ h$
K, half-saturation constant for R_1	$200\ \mu mol[C]\ L^{-1}$
D, dilution rate	$0.0083\ h^{-1}$ or $0.0062\ h^{-1}$
$\phi(t)$, cell-cycle parameter	adimensional
K_I, half-saturation constant	$55.5\ \mu mol\ quanta$ $m^{-2}\ s^{-1}$
K_{iI}, light-inhibition coefficient	$1500(\mu mol\ quanta$ $m^{-2}\ s^{-1})^2$

The parameter λ_6, representing the 'respiratory protection', has a stronger effect when photoperiod is longer, since photosynthesis and diazotrophy co-occur in this condition.

3. RESULTS AND DISCUSSION

3.1 Model simulation

The present model is designed to reproduce the observed, diel fluctuations in the carbon and nitrogen metabolism of *C. watsonii* when light limitation and obligate diazotrophy occur.

All model simulations are performed with the unique set of parameters obtained after calibration on the 12:12 LD experiment. Different runs are performed using successively the three light regimes as forcing conditions and results are then compared to experimental data obtained under the same three light regimes. The initial conditions for C_{tot}, N_{tot} and C_{st} are fixed to the corresponding experimental data, considering that total carbohydrates in cells can be used as first approximation of the initial C_{st}. Conversely, variables N_{st} and C_{nit}, for which there is no direct experimental match, can be initiated with a wider degree of freedom. Simulation are initiated at the beginning of a light period, assuming empty nitrogenase pool C_{nit} and nitrogen reserve N_{st}. The initial value of C_f is deduced from C_{st}.

The model reaches a periodic behavior in each simulation. Comparisons are made between total biomasses expressed as carbon (C_{tot} and POC) and nitrogen (N_{tot} and PON),

and between the measured cellular carbohydrates and the variable C_{st}. Results shown in Fig. 3 demonstrate that the model predicts the dynamics of cellular carbon, nitrogen and carbohydrates pools with fair accuracy. C_f and N_f pools are not compared to data but they participate to the correct C_{tot} and N_{tot} dynamics. The N_{tot}/C_{tot} ratio follows that observed experimentally. Thus, the accumulation or decrease of the carbon reserves C_{st} results from an imbalance between photosynthesis and carbohydrates consumption (through respiration and biosynthesis of structural components) and model results comply with the observation that carbon is stored during the photoperiod and largely consumed during the dark period to fuel diazotrophy.

The nitrogen inflow $\rho_1(C_{st}, C_{nit})$ compares well to the experimental nitrogenase activity (nitrogen fixed/L/h). Results (Fig. 2) show that the model, by taking into account the timing bracketed by the cell-cycle for nitrogen fixation, correctly reproduces the different patterns of nitrogenase activity observed under all light regimes.

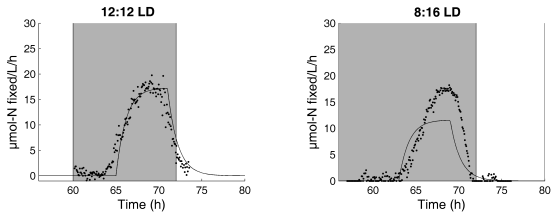

Fig. 2. Simulated (continuous line) and measured (dots) nitrogenase activity under the 12:12 LD and 8:16 LD light regimes, during 24 hours. White and grey backgrounds represent the light and dark periods, respectively.

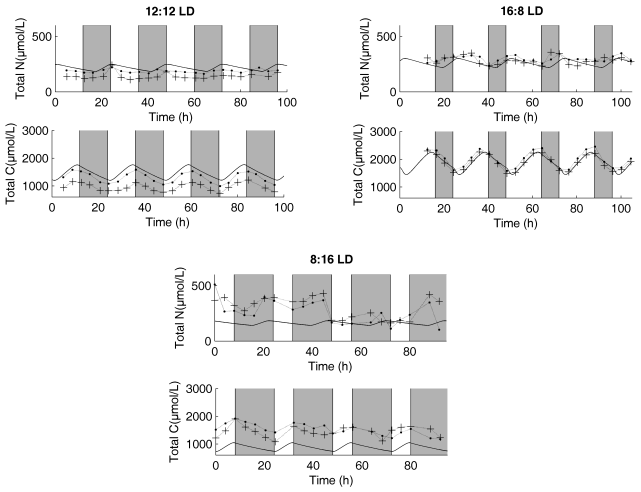

Fig. 3. Model simulation of C_{tot}, N_{tot}, C_{st} and C_{tot}/N_{tot} (continuous lines) compared to the experimental data of POC, PON, carbohydrates and PON/POC (dashed lines), respectively, under the three light regimes. The experimental duplicates are represented by closed circles and crosses. White and grey backgrounds represent the light and dark periods, respectively.

3.2 Influence of the photoperiod and light dose

In order to understand the role of photoperiodism on the dynamics of carbon and nitrogen metabolism in *C. watsonii*, the model is run for a range of photoperiods. First, we consider various photoperiods associated with the same daily light dose (3.743 mol quanta/m^2/d) corresponding to the 16:8 LD experiment. For each photoperiod, we use conditions obtained in the permanent regime after an initial transient as initial conditions for each run.

We quantify the carbon and nitrogen budgets for each photoperiod. We determine the total nitrogen fixed in N_{st} (gross) during 24 hours (N_{fixed}):

$$N_{fixed} = \int_0^{24} \rho_1\Big(C_{st}(t), C_{nit}(t)\Big)\,\mathrm{d}t \qquad (20)$$

Similary, we compare the total carbon stored into C_{st} (gross) during one day, CH_{fixed}, the total carbon integrated over one day, C_{tot_d} and the total nitrogen integrated over one day, N_{tot_d}.

Results, identify an optimal photoperiod of 14.5 h for N_{fixed}, 14 h for C_{tot} and N_{tot}, and 16 h for CH_{fixed}. Interestingly, optimal photoperiod for carbon and nitrogen acquisitions are very close. A balance between the quantity of carbohydrates stored and respired, depending upon the light-dark timing, explains this result. The amount of carbohydrates stored during the day depends on the photosynthesic activity $\rho_2(I(t), C_f)$.

To understand the additional effect of light dose, we combined simulations at different photoperiod length and daily light doses. We ran simulations from a daily light dose of 2 mol quanta m^2 d^{-1} to 60 mol quanta m^{2}d^{-1}.

The variables of interest are C_{tot}, N_{tot}, N_{fixed}, CH_{fixed}, estimated at steady-state (Fig.4). Simulations are performed with a dilution rate that equals the growth rate ($D = 0.0083$ h^{-1}). Results show that there is an optimal photoperiod/light intensity combination for all these variables: for example, a photoperiod comprised between 12 h and 15 h light and a daily light dose comprised between 7 mol quanta/m^2/d and 20 mol quanta/m^2/d for N_{fixed} (which is representative of the other variables).

The optimal duration of the light phase decreases with increasing irradiances. This phenomenon is due to the respiratory protection, which increases when photosynthesis increases, and by photoinhibition that limits growth at high light intensity.

4. CONCLUSION

We presented a dynamical growth model of a unicellular, diazotrophic cyanobacterium under light limitation and obligate diazotrophy. The model is successfully calibrated and validated against experimental data of *C.watsonii* exposed to different light-dark cycles. Simulations highlight how the carbon and nitrogen metabolism are tightly connected through the dynamics of carbohydrate reserves.

Simulations carried out with a range of light regimes and various photoperiods reveal the optimal photoperiod/intensity combination for the accumulation of carbohydrates and nitrogen.

ACKNOWLEDGEMENTS

This work was supported by the ANR Facteur 4 project and the LEFE-CYBER project CROCOCYCLE, the Con-

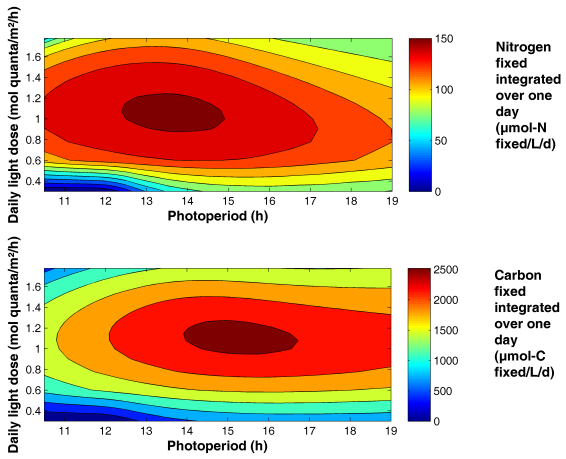

Fig. 4. Model simulation of the carbon fixed integrated over one day CH_{fixed} (top) and nitrogen fixed integrated over one day N_{fixed} (bottom) as a function of the daily light dose and photoperiod.

seil Régional des Alpes Maritimes and the Conseil Général PACA. We are grateful to Rafael Muñoz-Tamayo for his helpful suggestions concerning model calibration.

REFERENCES

Bastin, G. and Dochain, D. (1990). On-line estimation and adaptive control of bioreactors. In *Amsterdam*. Elsevier.

Carpenter, E. and Capone, D. (1992). Nitrogen fixation in *Trichodesmium* spp. in: Carpenter e.j., capone d.g. & rueter j. (eds) marine pelagic cyanobacteria: *Trichodesmium* and other diazotrophs. *Kluwer Academic Publishers, The Netherlands; Appl Environ Microbiol*, 211–217.

Carpenter, E. and Romans, K. (1991). Major role of the cyanobacterium *Trichodesmium* in nutrient cycling in the north atlantic ocean. *Science*, 254, 1356–1358.

Chow, T. and Tabita, F. (1994). Reciprocal light-dark transcriptional control of nif and rbc expression and light-dependent posttranslational control of nitrogenase activity in synechococcus sp strain rf-1. *Journal Of Bacteriology*, 176, 6281–6285.

Dron, A., Rabouille, S., Claquin, P., Chang, P., Raimbault, V., Talec, A., and Sciandra, A. (2012b). Light-dark (12:12) quantification of carbohydrate fluxes in *Crocosphaera watsonii*. *Aquat Micro Ecol*, DOI: 10.3354/ame01600.

Dron, A., Rabouille, S., Claquin, P., Le Roy, B., Talec, A., and Sciandra, A. (2012a). Light-dark (12:12) cycle of carbon and nitrogen metabolism in *Crocosphaera watsonii* wh8501: relation to the cell cycle. *Environ Microbiol*, 14, 967–981.

Dron, A., Rabouille, S., Claquin, P., and Sciandra, A. (2013). Photoperiod length paces the temporal orchestration of cell cycle and carbon-nitrogen metabolism in *Crocosphaera watsonii*. *Environ Microbiol*, doi: 10.1111/1462–2920.12163.

Goebel, N., Edwards, C., Carter, B., Achilles, K., and Zehr, J. (2008). Growth and carbon content of three different-sized diazotrophic cyanobacteria observed in the subtropical north pacific. *J Phycol*, 44, 1212–1220.

Grosskopf, T. and LaRoche, J. (2012a). Direct and indirect costs of dinitrogen fixation in *Crocosphaera watsonii* wh8501 and possible implications for the nitrogen cycle. *Frontier in Microbiology*, 3, 1–10.

Han, B.P. (2001). Photosynthesis-irradiance response at physiological level: A mechanistic model. *J. Theor. Biol.*, 213, 121–127.

Karl, D., Michaels, A., Bergman, B., Capone, D., Carpenter, E., Letelier, R., Lipschultz, F., Paerl, H., Sigman, D., and Stal, L. (2002). Dinitrogen fixation in the world's oceans. *Biogeochemistry*, 57, 47–98.

Lee, K., Karl, D., Wanninkhof, R., and Zhang, J. (2002). Global estimates of net carbon production in the nitrate-depleted tropical and subtropical oceans. *Geophys Res Lett*, 29, 257–268.

Li, H., Sherman, D., Bao, S., and Sherman, L. (2001). Pattern of cyanophycin accumulation in nitrogen-fixing and non-nitrogen-fixing cyanobacteria. *Arch Microbiol*, 176, 9–18.

Long, S.P., Humphries, S., and Falkowski, P.G. (1994). Photoinhibition of photosynthesis in nature. *Annual Review of Plant Biology*, 45, 633–662.

Mairet, F., Bernard, O., Masci, P., Lacour, T., and Sciandra, A. (2010). Modelling neutral lipid production by the microalga *Isochrysis* aff. *galbana* under nitrogen limitation. *Bioresource Technology*, 102, 142–149.

Mitsui, A., Kumazawa, S., Takahashi, A., Ikemoto, H., Cao, S., and Arai, T. (1986). Strategy by which nitrogen-fixing unicellular cyanobacteria grow photoautotrophically. *Nature*, 323, 720–722.

Muñoz Tamayo, R., Laroche, B., Leclerc, M., and Walter, E. (2009). Ideas: a parameter identification toolbox with symbolic analysis of uncertainty and its application to biological modelling. *15th Symposium on System Identification*.

Mulholland, M., Bronk, D., and Capone, D. (2004). Dinitrogen fixation and release of ammonium and dissolved organic nitrogen by *trichodesmium* ims101. *Aquat Microb Ecol*, 37, 85–94.

Rabouille, S., Staal, M., Stal, L., and Soetaert, K. (2006). Modeling the dynamic regulation of nitrogen fixation in the cyanobacterium *Trichodesmium* sp. *Appl Environ Microbiol*, 72, 3217–3227.

Robson, R. and Postgate, J. (1980). Oxygen and hydrogen in biological nitrogen-fixation. *Annu Rev Microbiol*, 34, 183–207.

Ross, O. and Geider, R. (2009). New cell-based model of photosynthesis and photo-acclimation: accumulation and mobilisation of energy reserves in phytoplankton. *Mar Ecol Progr Ser*, 383, 53–71.

Waterbury, J. and Rippka, R. (1989). Cyanobacteria. subsection i. order chroococcales. *In Bergey's Manual of Systematic Bacteriology, Krieg, N.R., and Holt, J.B. (eds). Baltimore, MD, USA: Williams and Wilkins*, 3, 1728–1746.

Zehr, J., Tripp, H., Hilton, J., Moisander, P., and Foster, R. (2011). Ecological aspects of nitrogen-fixing cyanobacteria illuminated by genomics and metagenomics. *Journal of Phycology*, 47, S1–S1.

Zehr, J., Waterbury, J., Turner, P., Montoya, J., Omoregie, E., Steward, G., and al. (2001). Unicellular cyanobacteria fix n_2 in the subtropical north pacific ocean. *Nature*, 412, 635–638.